Chem. Senses 37: 35–46, 2012

doi:10.1093/chemse/bjr063
Advance Access publication July 10, 2011

Aquaporin Pathways and Mucin Secretion of Bowman's Glands Might Protect the Olfactory Mucosa

Tom T. Solbu and Torgeir Holen

Department of Anatomy, Institute of Basic Medical Sciences, Sognsvannsveien 9, University of Oslo, 0317 Oslo, Norway

Correspondence to be sent to: Torgeir Holen, Department of Anatomy, Institute of Basic Medical Sciences, University of Oslo, PO Box 1110, Blindern, 0317 Oslo, Norway. e-mail: torgeir.holen@medisin.uio.no

Accepted June 9, 2011

Abstract

The sense of smell is conveyed by the olfactory sensory neurons of the olfactory mucosa. Uniquely for sensory systems, the olfactory neurons directly face the external environment and are thus vulnerable to infections and changes in the airway surface liquid, but the surface liquid production and maintenance is not well understood. Here we show in rats and mice that Bowman's glands secrete the mucin MUC5AC. Aquaporin-5 was present at the apical face of the olfactory epithelium, completing a water transport pathway to the surface of the epithelium. Immunogold electron microscopy analysis revealed an intricate network of fine Aquaporin-1–positive fibroblast processes that surround Bowman's glands, whereas deeper blood vessels were unlabeled for Aquaporin-1. Our results show how the olfactory mucosa might be protected against infections and dehydration generally and how neuronal function is protected against ion concentration changes in the airway surface liquid by rapid replacement of water losses through the aquaporin pathways.

Key words: airway surface liquid, electron microscopy, olfactory mucosa

Introduction

The olfactory mucosa with its Bowman's glands is situated in the dorsal and caudal nasal cavity (Todd and Bowman 1847; Köllicker 1855). Despite a long history of investigation, the function of Bowman's glands and several aspects of the olfactory mucosa liquid secretion and maintenance are still unsettled. The nasal cavity is lined with ciliated respiratory epithelium containing mucus-secreting goblet cells, whereas the respiratory submucosal glands are not open to the immediate local surface (Bojsen-Moller 1964). The olfactory epithelium lacks goblet cells, and only the olfactory neurons have cilia, which are non-motile. In humans, when olfactory epithelium is gradually lost by age, or infection, also Bowman's glands are lost or disrupted along with the olfactory epithelium (Nakashima et al. 1984). Published data on the olfactory mucosa of the important rodent animal models mouse and rat are rather scarce, in particular ultrastructural analysis (Frisch 1967; Seifert 1971; Breipohl 1972). The exact molecular identity of Bowman's glands secretion products have remained unknown, although histochemical studies showed that Bowman's glands in rats are positive for periodic acid–Schiff (PAS) staining, indicative of neutral glycoproteins (Bojsen-Moller 1964; Katz and Merzel 1977). A more comprehensive study in mice also found evidence for sulfated glycoproteins (Cuschieri and Bannister 1974).

The utility of light microscopy analysis is limited by the complex character of olfactory mucosa, with its interwoven tissues of glands, blood vessels, connective tissue cells and large, converging bundles of olfactory sensory neuron axons penetrating into the bone of the cribriform plate. Electron microscopy studies in different species have observed two types of secretory vesicles in Bowman's glands. Large, electron-lucent vesicles are found in dark cells and smaller, electron-dense vesicles in light cells (Frisch 1967; Seifert 1971; Breipohl 1972). Studies from a variety of animal models indicate that the content of the electron-lucent secretory vesicles are mucous glycoproteins, whereas the electron-dense vesicles are proteinaceous and serous (Getchell and Getchell 1992).

Mucins, a glycoprotein family that historically have been difficult to isolate and characterize, can now be investigated due to advances in bioinformatics and transgenic techniques. Recently, the mucin gene family has been extensively investigated in the lower respiratory tract in humans (Rose and

© The Author 2011. Published by Oxford University Press. All rights reserved.
For permissions, please e-mail: journals.permissions@oup.com

Downloaded from http://chemse.oxfordjournals.org/ at Changhua Christian Hospital on October 6, 2012

Voynow 2006). The glycoproteins of the mucin family would be promising candidates for the secretory components of Bowman's glands, but so far mucins have not been characterized in the olfactory mucosa and few mucin antibodies are presently available for rodent models.

Strong expansion of mucins (>100-fold) after fast secretion (Kamijo et al. 1993; Rogers 1994) probably requires a fast water supply, a role for which the water channel family of aquaporins is well adapted. Proper function of mucous membranes are known to require coordinated cotransport of water and ions, as exemplified by overproduction of viscous mucus in the cystic fibrosis syndrome (Jayaraman et al. 2001), and hypertonic and viscous secretion from the salivary glands of the aquaporin-5 knockout mice (Ma et al. 1999).

The expression profile of aquaporins (AQP) in the olfactory epithelium is markedly different from the respiratory epithelium, as shown by immunohistochemistry in rat models (Nielsen et al. 1997a; Ablimit et al. 2006; Sorbo et al. 2007), indicating different water transport requirements of these two tissues. As AQP4 is strongly present in Bowman's glands (Nielsen et al. 1997a; Ablimit et al. 2006; Sorbo et al. 2007), it is notable that AQP4 knockout mice are deficient in olfaction (Lu et al. 2008).

Here we characterize rat and mice Bowman's glands, olfactory and respiratory mucosa, using classical histological stains for mucous glands, immunohistochemistry, and novel immunogold electron microscopy techniques for the nasal cavity in order to study mucin expression and the exact cellular and subcellular location of aquaporin water pathways.

We find that rodent Bowman's glands are exclusively mucous using PAS and Alcian Blue (AB) stains and electron microscopy. MUC5AC, a secreted glycoprotein, was found to be present in the ducts of Bowman's glands, in secretory vesicles, and in the mucous layer at the top of the epithelium. The aquaporin AQP5 was found apically in the olfactory epithelium, thus making possible a water pathway through the olfactory epithelium, whereas immunogold electron microscopy analysis demonstrated a water pathway from AQP1-containing blood vessels through AQP1-positive fibroblasts that surround each Bowman's gland. Together the mucin secretion and aquaporin pathways suggest how the olfactory mucosa is protected against infection and dehydration.

Materials and methods

Animals and AQP4 knockout animals

Experimental protocols were approved by the Institutional Animal Care and Use Committee and conform to National Institutes of Health guidelines for the care and use of animals. Studies were conducted with male BN rats (Charles River, Germany). Mice homozygous for targeted disruption of the gene encoding AQP4 (Thrane et al. 2011) and control wild-type C57Bl/6 mice were used.

Tissue preparation and antibody staining for light microscopy

Rats and mice were perfusion fixated with 4% paraformaldehyde (PFA). The nasal region was dissected and post-fixed over night in 4% PFA and then decalcinated for 24 h in 10% formic acid. Tissues were then cryoprotected in 30% sucrose before sectioning with a Leica CM3050 S cryostat.

Immunoperoxidase and immunofluorescence staining was carried out with the biotin–streptavidin–peroxidase/DAB system and immunofluorescence-coupled secondary antibodies, respectively. All pictures were acquired using Zeiss LSM PASCAL Axioplan 2 Imaging confocal microscope.

Antibodies

The antibodies are summarized in Table 1. Affinity-purified rabbit AQP1 antibody was a gift from Soren Nielsen (Nielsen et al. 1993). The AQP3 antibody was purchased from Sigma (cat no.: A0303, lot no. 048k1363). An AQP4 antibody from Santa Cruz Biotechnology (SC9888) was used for light microscopy. For electron microscopy, two AQP4 antibodies were used (cat no. A5971, lot no. 116K1630, Sigma; and LS-C3805, lot no. 7091355, LifeSpan Biosciences). An AQP5 antibody was purchased from Calbiochem

Table 1 Antibody overview

Antigen	Immunogen	Species	Source
AQP1	Purified protein	Rabbit	S. Nielsen (Nielsen et al. 1993)
AQP3	aa 275–292 (C-terminus) affinity purified	Rabbit	Sigma A0303
AQP4	C-terminus, affinity purified	Goat	Santa Cruz SC-9888
AQP4	aa 249–323 (C-terminus) affinity purified	Rabbit	Sigma A5971
AQP4	aa 280–296, affinity purifie	Rabbit	Life Sciences LS-C3805
AQP5	17 aa in C-terminus	Rabbit	Calbiochem #178615
AQP5	RaTM14 (aa 251–265)	Rabbit	T. Matsuzaki (Ablimit et al. 2006)
AQP5	RaTM41 (aa 244–257)	Rabbit	T. Matsuzaki (Ablimit et al. 2006)
CFTR	N-terminus	Goat	Santa Cruz SC-8909
Golf	Aa 82–381 (C-terminus) monoclonal	Mouse	Santa Cruz SC-55545
MUC5AC	Recombinant Mucin 5AC protein monoclonal	Mouse	Lab Vision MS-10331-P0

Downloaded from http://chemse.oxfordjournals.org/ at Changhua Christian Hospital on October 6, 2012

(cat. no.:178615, lot no.D00036895). The AQP5 antibodies RaTM14 and RaTM41 were gifts from Toshiyuki Matsuzaki (Matsuzaki et al. 2006). The MUC5AC antibody (cat no. MS-10331-P0, lot no.10331P903G) was purchased from Thermo Scientific Labvision. The Golf antibody was purchased from Santa Cruz (cat no. sc-55545, lot no. B2307).

Immunogold electron microscopy

Rats and mice were perfusion fixated with 4% PFA and 0.1% glutaraldehyde. Nasal tissues were dissected and post-fixed overnight in the same fixative solution and then decalcinated 24 h in 10% formic acid. Tissue samples were then dissected out, and the specimens were cryoprotected by immersion in graded concentrations of glycerol (10%, 20%, and 30%) and plunged rapidly into liquid propane (170 °C) cooled by liquid nitrogen in a cryofixation unit (KF 80; Reichert). The samples were immersed in 1.5% uranyl acetate dissolved in anhydrous methanol (90 °C, 24 h) in a cryosubstitution unit (AFS; Reichert). The temperature was raised in steps of 4 °C/h from 90 to 45 °C. The samples were washed with anhydrous methanol and infiltrated with Lowicryl HM20 resin at 45 °C with a progressive increase in the ratio of resin to methanol. Polymerization was carried out with ultraviolet light (360 nm) for 48 h.

Ultrathin sections (80 nm) were washed with low saline Tris-buffered saline with Tween-20 (TBST) (LS-TBST) containing 0.05 M Tris-HCl, pH 7.4, 0.4% NaCl, and 0.2% Triton X-100 and incubated in TBST with 50 mM glycine for 10 min before blocking and subsequently incubation over night with antibody. Blocking buffer and incubation buffer used was LS-TBST with 2% human serum albumin (HSA). Sections were then washed in LS-TBST before incubation for 60 min with secondary gold-conjugated antibodies from Abcam, used at 1:20 dilution in LS-TBST with 2% HSA and 0.5 mg/ml polyethylene glycol. The size of gold particles used was 15 nm in all experiments. Sections were finally washed in water and dried before contrasting in 2.7% lead citrate. Sections were then washed and dried again before contrasting in 2% uranyl acetate for 90 s.

Results

The olfactory mucosa is situated dorsally and caudally in the nasal cavity on, or in proximity to, the cribriform plate. The olfactory epithelium is wide and pseudostratified, with a sharp transition to the narrow respiratory epithelium (Figure 1A, arrows). The submucosal Bowman's glands are situated in the lamina propria, with ducts penetrating to the olfactory epithelium surface (Figure 1A, box III). The large, complex nasal glands of the septum (Figure 1A, box II) and lateral wall glands, in contrast, do not connect to the immediate surface but secrete via duct systems to the nasal vestibule (Tandler and Bojsen-Moller 1978; Klaassen et al. 1981). Some dorsal maxillary glands exit locally into the maxillary sinus, whereas ventral maxillary glands (Figure 1A, arrowheads) do not (Klaassen et al. 1981).

We investigated the rat olfactory mucosa with classic stains, finding that Bowman's glands were both PAS positive (Figure S1A), consistent with two previous reports (Bojsen-Moller 1964; Katz and Merzel 1977), and AB positive, indicative of the presence of acidic glycoproteins (Figure S1B). Thus, rat Bowman's glands are mucous, with both neutral and acidic glycoproteins present. As controls, goblet cells of the respiratory epithelium and septal glands were found to be PAS positive, whereas ventral maxillary sinus glands were also AB positive.

Aquaporin-5 expression on the apical face of the olfactory epithelium

The Bowman's glands and ducts are known to express AQP4 distinctly stronger than in the olfactory epithelium itself (Figure S2A; Nielsen et al. 1997a; Ablimit et al. 2006; Sorbo et al. 2007; Lu et al. 2008). At the junction between respiratory epithelium and olfactory epithelium, AQP3 can be demonstrated to be expressed strongly in the olfactory epithelium (Figure S2B, red staining). AQP4 expression, on the other hand, is much stronger in the respiratory epithelium (Figure S2B and Figure 1B, green staining).

Surprisingly, AQP5, previously known to be present apically in Bowman's gland ducts (Nielsen et al. 1997a; Ablimit et al. 2006), was found to be also expressed at the surface of the olfactory epithelium (Figure 1B, red staining). The olfactory epithelium AQP5 staining was consistent at all tissue junctions, both at the septum and at ethmoidal turbinates. The AQP5 staining pattern was replicated in sections from several different animals and with different staining methodology (Figure 1A, DAB staining). Yet further controls were instituted by obtaining another two AQP5 antibodies used by Ablimit et al., both of which yielded consistent results, with both rat and mouse sections (Figures S2C,D). Double labeling with the !olfactory sensory neuron cilia marker Golf (Menco et al. 1992), and AQP5, demonstrated that AQP5 is not present in the cilia (Figure 1C). The discovery of AQP5 expression at the apical side of olfactory epithelium completes a potential water transport pathway across this epithelium and further supports the hypothesis of different water transport requirements of the olfactory and respiratory epithelial tissues.

Although the structure of Bowman's ducts are easily observable in the olfactory epithelium, the complex, convoluted character of the lamina propria (Figure 3A, below) makes the light microscopy visualization of distinct Bowman's glands and ducts difficult. However, using confocal images of AQP5, from a series of planes, and combining these images into a Z-stack projection over 20 μm, enhances signal strength and reveals the nonbranched, simple tubular structure of Bowman's glands (Figure 1D).

In submucosal glands in the lower respiratory tract, the cystic fibrosis transmembrane conductance regulator protein (CFTR), a chloride channel at the apical side of secretory

Downloaded from http://chemse.oxfordjournals.org/ at Changhua Christian Hospital on October 6, 2012

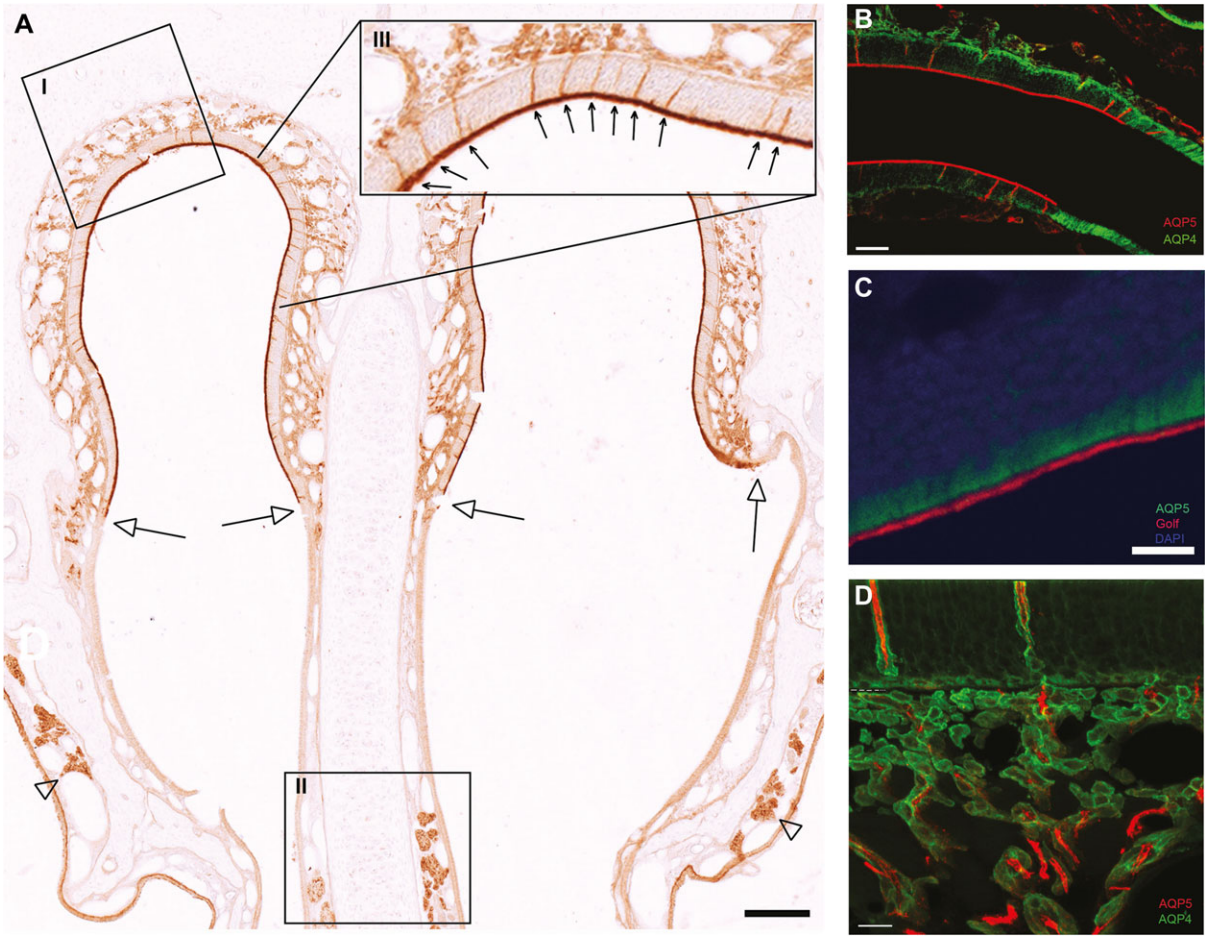

Figure 1 Aquaporin-5 expression in olfactory mucosa **(A)** Overview of olfactory and respiratory mucosa at low magnification. Coronal section of nose tissues, with olfactory mucosa (dorsal) and respiratory mucosa (ventral). Arrows indicate transition from olfactory epithelium to respiratory epithelium. Arrowheads point to lateral nasal glands of the maxillary sinus. Box I indicates olfactory mucosa, close to the cribriform plate, sampled for electron microscopy. Box II indicates region sampled for electron microscope analysis of the septal glands and respiratory epithelium. Box III is high magnification of olfactory mucosa, visualizing Bowman's ducts and apical labelled Bowman's glands stained for AQP5. Scale bar 500 μm. **(B)** Double labelling of olfactory (left) and respiratory mucosa (right) with AQP4 (green) and AQP5 (red). Scale bar 100 μm. **(C)** Double labelling of Golf (red) and AQP5 (RaTM41 antibody [green]), in olfactory epithelium, with DAPI staining (blue). Scale bar 20 μm. **(D)** Higher magnification and z-stack enhancement of olfactory epithelium (top) and lamina propria (bottom) double labeled for AQP4 (green) and AQP5 (red). Dotted line indicates the orientation of basal lamina (white, left). Scale bar 20 μm.

cells, regulates secretion (Song and Verkman 2001). Although septal nasal gland ducts exhibited strong apical staining for CFTR (Figure S2E), CFTR was absent from Bowman's glands, thus the driving force for Bowman's gland secretion remains unknown.

Mucin secretion by Bowman's glands

Classical mucous stains (Figures S1A,B) and electron microscopy (see below) indicate that Bowman's glands secretory products are mucous glycoproteins. The mucin gene family has been investigated in lower respiratory tract in humans and in some studies of rodent airways, conjunctiva, and intestines (Rose and Voynow 2006). Testing the available rat and mouse antibodies, we found that MUC5AC was present in the olfactory mucosa (Figure 2A). The presence of MUC5AC as a secretion product lying on top of the epithelium is also indicated from the preparatory loss of the mucus layer in some spots (Figure 2A, left). Double labeling of AQP5 and MUC5AC further demonstrated that MUC5AC was separate from the epithelium (Figure 2B). With higher magnification, MUC5AC could be seen in Bowman's ducts traversing the epithelium, in ducts in the lamina propria and also as speckles inside AQP4-positive cells, indicative of secretory vesicles (Figure 2C).

The ultrastructure and immunogold AQP4 analysis of olfactory mucosa

Due to the limited resolution by light microscopy techniques, and the complex character of the lamina propria, we set up ultrastructural methods for analyzing olfactory mucosa and Bowman's glands. Using Lowicryl HM20–embedded olfactory mucosa from the cribriform plate and dorsal septum

Downloaded from http://chemse.oxfordjournals.org/ at Changhua Christian Hospital on October 6, 2012

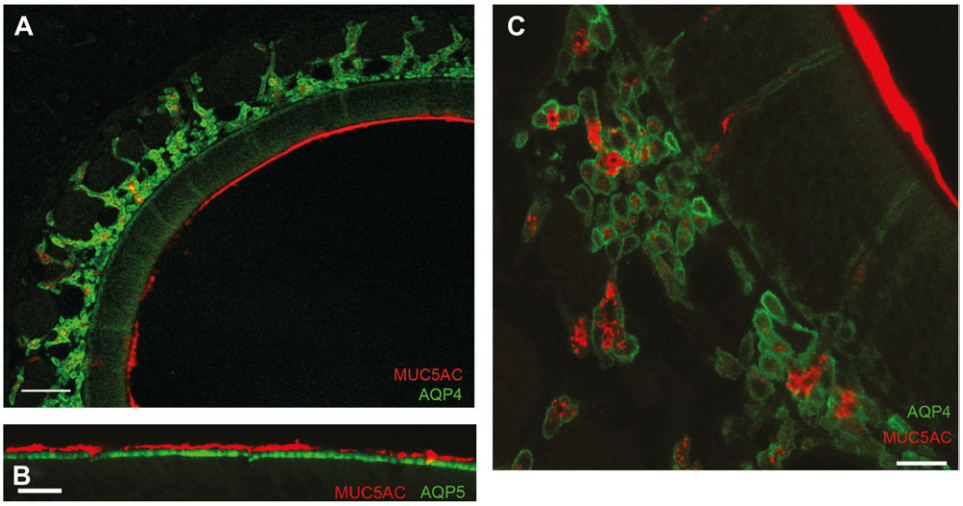

Figure 2 Mucin expression in olfactory mucosa. **(A)** Overview of olfactory mucosa with double labeling for AQP4 (green) and MUC5AC (red). Scale bar 100 μm. **(B)** High magnification of epithelial surface with double labeling of MUC5AC (red) and AQP5 (green). Scale bar 20 μm. **(C)** High magnification of double labeling with AQP4 (green) and MUC5AC (red). Scale bar 20 μm.

(Figure 1A, box I), Bowman's glands appear under electron microscopy analysis to be organized as acinar clusters of cells around a central lumen (Figure 3A, L1). The crowded character of the lamina propria is apparent by the Bowman's glands being surrounded by multiple bundles of olfactory neuron axons (AB1–AB4), in which the nuclei of olfactory ensheathing cells are situated, and a capillary (V). Present are also fibroblasts (FN) and several other Bowman's glands (L2–L4). Between the cells, large bundles of collagen can be seen. The Bowman secretory cells are generally dark, with clusters of large, electron-lucent secretory vesicles localized at the apical pole close to the lumen (L1–L4). The nucleus of the Bowman's gland cell is situated at the basal pole of the cells (N), and often presents with a characteristic mix of dark speckles, representing heterochromatin. Few microvilli are seen in the central lumen of rat Bowman's glands.

We have here improved upon a technique that combines good ultrastructure of the nasal cavity with quantitative detection and localization of specific antigens. Lowicryl embedding of tissues facilitates quantitative post-embedding immunogold detection of proteins with antibodies (Chaudhry et al. 1995). However, not all antibodies prove suitable for the immunogold technique, for reasons that are not clear. For AQP4 immunogold studies in the brain, antibodies that have been utilized with success are no longer available (Nielsen et al. 1997b). The two new commercially available AQP4 antibodies used have been validated on brain tissues. Mucin antibodies and several other antibodies tested proved unsuitable for EM analysis. It should be noted that olfactory mucosa embedded in Lowicryl HM20 proved to be much more vulnerable to the electron beam than brain and respiratory mucosa sections.

The gold particles representing AQP4 were situated densely at the basolateral membranes of Bowman's gland cells (Figure 3B). The endothelial cell body and nucleus, fibroblast processes, and collagen had very little or no labeling, indicating excellent specificity of the Sigma AQP4 antibody. Also the Bowman cell secretory vesicles were free of immunogold labeling (Figure 3B, upper left). Control experiments using olfactory mucosa tissue samples from AQP4 knockout mice showed no labeling (Figure 3C), further demonstrating high antibody specificity. The Bowman's glands from the AQP4 knockout mouse exhibited no obvious morphological changes from the wild-type mouse. All observations on wild-type mice were consistent with results in rats, although dark speckles inside the rat secretory vesicles were generally less prominent in mice. Control experiments with a second AQP4 antibody from LifeSpan Biosciences showed the same expression patterns.

AQP4 was present at the lateral sides of the Bowman cells, penetrating toward the lumen (Figure 3D, right) but were clearly excluded by the tight junction zone near the lumen (Figure 3D, left). The luminal side of the secretory cells was always free of AQP4 labeling. Usually very few microvilli were seen in the rat lumen, which is consistent with a previous ultrastructural study in mice (Frisch 1967). An earlier report indicated nonoverlapping sets of AQP4 and AQP3 staining (Nielsen et al. 1997a). No Bowman's glands' cells were found without AQP4 staining, although there might be a tendency of deeper glands to have less AQP4 staining than glands closer to the epithelium.

The basal lamina separating rat olfactory epithelium from the lamina propria was sometimes visible as a fine band (Figure 3E, arrowhead) situated next to a layer of supporting collagen (Figure 3E, right). No basal lamina was observed around Bowman's glands, which contrasts with the general association of AQP4 with the basal lamina in brain tissues (Nielsen et al. 1997b), indicating that AQP4 anchoring (Neely et al. 2001; Madrid et al. 2001) might be different in Bowman's glands.

Downloaded from http://chemse.oxfordjournals.org/ at Changhua Christian Hospital on October 6, 2012

The Bowman duct lumen in the epithelium had many microvilli (Figure 3E), in contrast with the scarcity of microvilli in the lumen in the lamina propria. The presence of many microvilli in the duct lumen would increase the total surface and thus could further facilitate ion and water transport laterally from the epithelial cells into the duct lumen. There was strong AQP4 labeling on the lateral side of the duct cells (Figure 3E, arrows), whereas the duct lumen and the microvilli were free of labeling.

Secretory vesicles were present in cells in the epithelial layer, something that has been observed also in mice (Frisch 1967). However, secretory vesicles in the epithelial layer were only observed in cells close to the basal lamina and not in the duct cells closer to the surface of the epithelium. At the basal lamina, the epithelial layer ended in a convoluted mixture of processes that were labeled for AQP4 but which seldom could be followed to a cell soma. The presence of AQP4 in the basal cell layer has been observed previously by light microscopy (Ablimit et al. 2006; Sorbo et al. 2007). AQP4 expression in the basal cell layer processes indicates that AQP4 participates in the water pathway supplying the olfactory mucosa surface and ducts.

In all Lowicryl-embedded material, from rats and wild-type and AQP4-KO mice, the Bowman's glands secretory vesicles appeared large and electron lucent and in no cases were serous vesicles of the electron-dense kind observed.

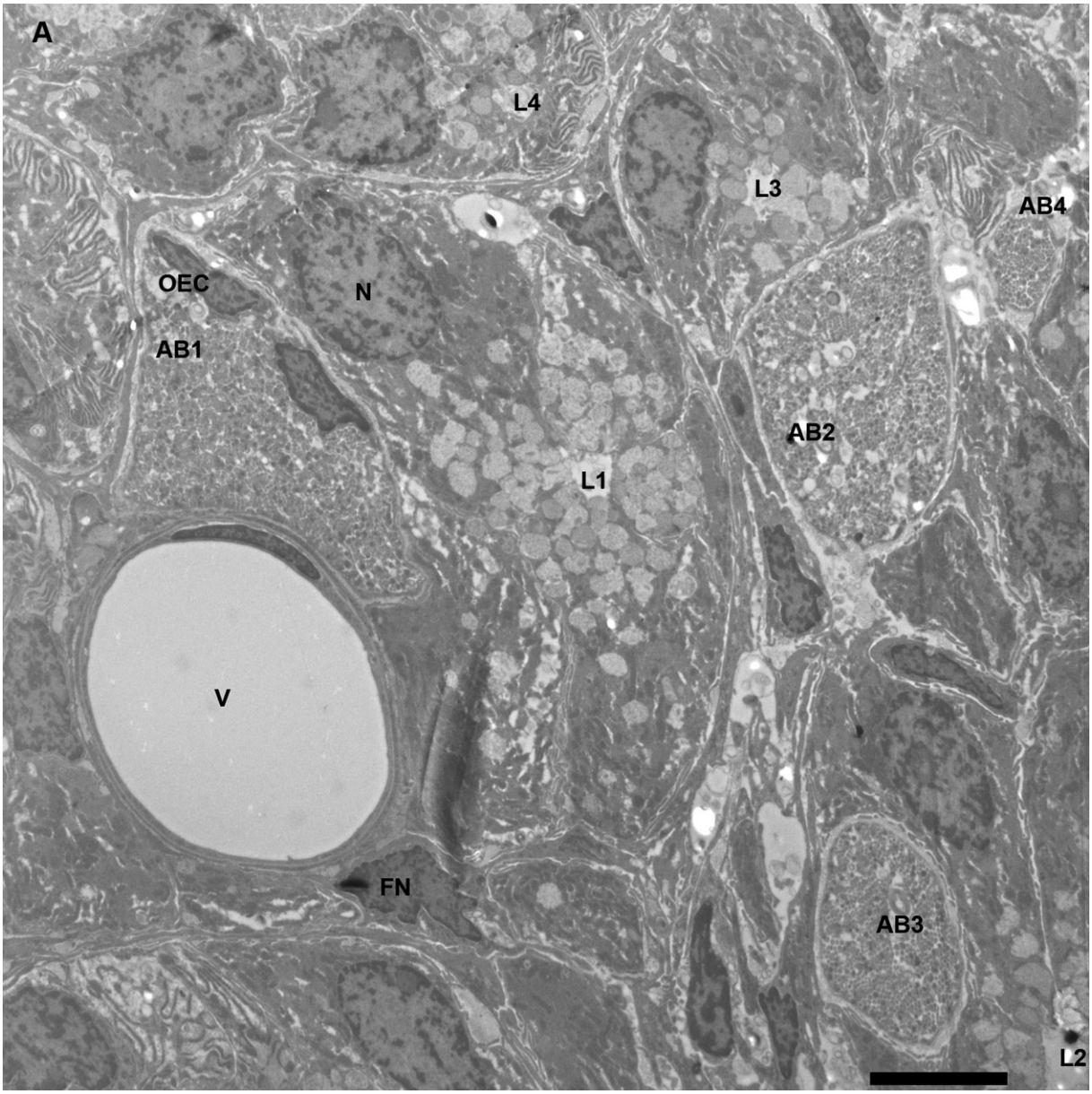

Figure 3 continued

Downloaded from http://chemse.oxfordjournals.org/ at Changhua Christian Hospital on October 6, 2012

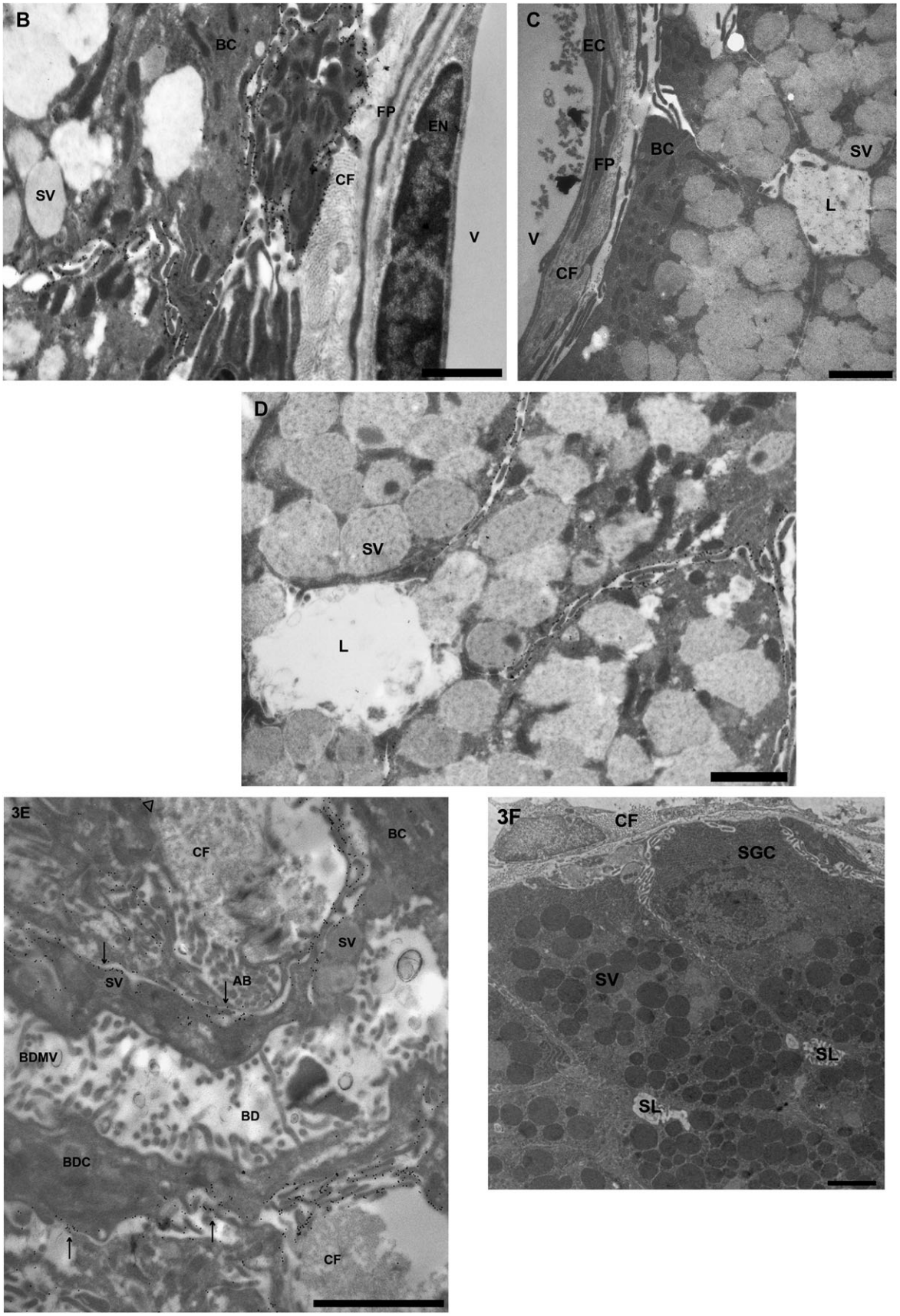

Figure 3 Continued

Downloaded from http://chemse.oxfordjournals.org/ at Changhua Christian Hospital on October 6, 2012

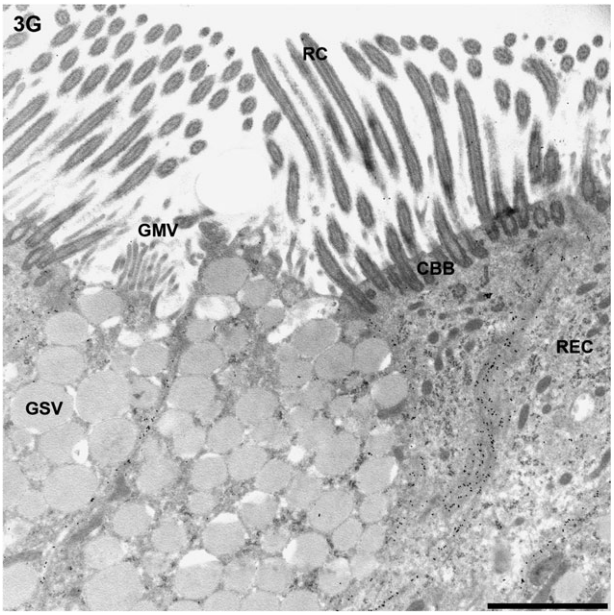

Figure 3 Electron microscopy analysis of olfactory and respiratory mucosa. AB, AB1–AB3, axonal bundles; BC, Bowman gland cell; BD, Bowman gland duct; BMV, Bowman gland cell microvilli; BDC, Bowman gland duct cell; BDMV, Bowman duct microvilli; CBB, ciliary basal bodies; CF, collagen fibers; EN, endothelial nucleus; EC, endothelial cell; FN, fibroblast nucleus; FP, fibroblast process; GC, septal gland cell; GSV, goblet cell secretory vesicle; GMV, goblet cell microvilli; L, L1–L4, Bowman's gland lumens; M, mitochondrium; N, Bowman's gland secretory cell nucleus; OEC, olfactory ensheathing cell nucleus; ONF, olfactory neuron fibroblast process; RC, respiratory epithelium cilia; REC, respiratory epithelial cell; SL, septal gland lumen; SV, secretory vesicle; V, capillary blood vessel. Pale collagen can also be seen and the occasional lacuna caused by electron beam damage. **(A)** Electron microscopy overview of Bowman's glands in the complex environment of the lamina propria. Scale bar 5 μm. **(B)** High-resolution immunogold staining for AQP4 at the basolateral surface of a Bowman gland. Scale bar 1 μm. **(C)** Bowman's glands in an AQP4 knockout mouse. No gold labeling for AQP4 is seen. Scale bar 2 μm. **(D)** Analysis of Bowman's gland lumen and AQP4 staining exclusion at the zonula occludens. Scale bar 1 μm. **(E)** Bowman duct crossing basal lamina and collagen layer (center and right) into the olfactory epithelium (left). Strong AQP4 staining is seen on the lateral side of the duct cells (arrows). Scale bar 2 μm. **(F)** Electron-dense secretory vesicles of septal nasal glands cells. Not immunogold labeled. Scale bar 2 μm. **(G)** Analysis of goblet cells and epithelial cells of the septal respiratory epithelium. A pair of goblet cells with electron-lucent secretory vesicles and microvilli at the apical face is seen to the left. A pair of respiratory epithelial cells with long, protruding cilia is seen to the right. AQP4 staining is present at the lateral sides of the goblet and epithelial cells but less abundant between the goblet cells pairs and absent from the apical face and the cilia of the respiratory epithelium. Scale bar 1 μm.

In order to control for possible methodological limitations with Lowicryl HM20 embedding, we undertook a study of septal and lateral wall respiratory mucosa, which are known to contain serous glands. The secretory vesicles of the nasal glands of the septum were found to be of the electron-dense, dark kind (Figure 3F), thus validating our observation of a lack of serous glands in rat and mouse olfactory mucosa.

The goblet cells of the respiratory epithelium exhibited electron-lucent vesicles similar to Bowman's glands (Figure 3G). No aquaporin has been identified at the luminal side of the respiratory epithelium despite strong presence at the basolateral side (Nielsen et al. 1997a; Ablimit et al. 2006; Sorbo et al. 2007). No AQP4 labeling was seen at the apical face (Figure 3G). As Bowman's glands exhibit an obvious water pathway into the secretory cells, a possibility existed that water is cotransported with goblet cell mucus in the respiratory epithelium. However, AQP4 labeling of goblet cells was distinctly weaker than the surrounding ciliated epithelial cells. Quantitative analysis of 13 goblet cell pairs found the density to be ~4.9 immunogold particles (imgp) per micrometer, whereas the density between respiratory epithelial cells were ~18.4 imgp/μm. The 3.8-fold higher AQP4 levels in respiratory epithelial cells would seem to argue that goblet cells have lower water transport needs than the surrounding respiratory cells and that water transport to the respiratory epithelial surface is thus not through goblet cells. Possibly, the large surface of cilia of the epithelial cells would allow sufficient water transport across the lipid bilayer by diffusion alone or that the aquaporins serve in cell volume regulation in connection with nasal erectile tissue activity.

Ultrastructural analysis of AQP1-positive fibroblasts and endothelial cells

Aquaporin-1 is the main aquaporin in the proximal tubules of the kidneys, erythrocytes, and endothelium (King et al. 2004). In the brain, AQP1 is absent from endothelium but present in the choroid plexus of the ventricles (Nielsen et al. 1993). In olfactory mucosa, two separate groups have

Downloaded from http://chemse.oxfordjournals.org/ at Changhua Christian Hospital on October 6, 2012

observed AQP1 using light microscopy (Nielsen et al. 1997a; Ablimit et al. 2006).

The AQP1 antibody proved to demonstrate strong immunogold labeling of endothelial cells and fibroblasts in the lamina propria of the olfactory mucosa (Figure 4A). The collagen fibrils (Figure 4A, center) and Bowman cells (Figure 4A, right) were unlabeled, showing that the AQP1 antibody exhibits little background labeling. The strong presence of AQP1 in the endothelial cells and intermediate fibroblasts close to the Bowman cell could indicate that a fast, transcellular fibroblast pathway exists for water transport into the Bowman's glands.

A systematic study of fibroblasts using high-magnification electron microscopy demonstrated strong expression of AQP1 in ~50-nm diameter processes of the fibroblasts, processes almost as thin as collagen fibers (Figure 4B) and distinctly thinner than the ~200-nm diameter olfactory sensory neuron axons. Collagen fibers, seen both in cross section (Figure 4B, center) and longitudinal section (Figure 4B, upper right), demonstrate the considerable resolution possible using Lowicryl HM20-embedding EM. The collagen fibers also indicate that olfactory mucosa would be able to resist tension. Whether olfactory mucosa exhibits regulated swelling and shrinkage similar to other nasal erectile tissues is not known. Possibly, the continual turnover and regrowth of the olfactory sensory neuron axons through the lamina propria and into the brain (Schwob 2002) also necessitates flexibility.

Fibroblasts with strong AQP1 expression were not only present around blood vessels (Figure 4C, right) but seemed to penetrate into the tissue and envelope Bowman's glands (Figure 4C, left). The dark, fine processes of fibroblasts penetrating into the tissue could be followed for considerable distances away from the blood vessels. In no cases were AQP1 labeling of axonal bundles seen (Figure 4C, upper

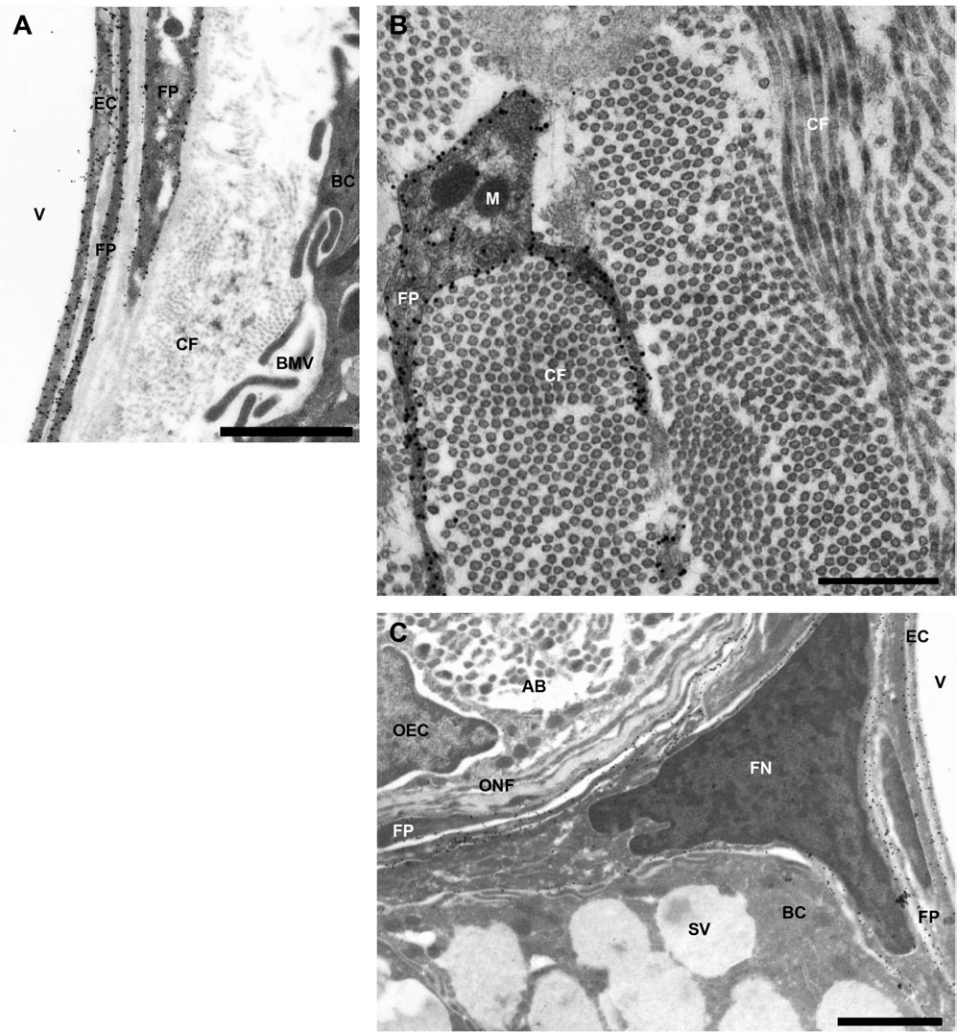

Figure 4 Immunogold electron microscopy analysis of AQP1 expression in olfactory mucosa. Abbreviations as in Figure 3. **(A)** Analysis of AQP1 expression in large, superficial venules. Scale bar 1 μm. **(B)** High resolution of fibroblast processes and collagen. Scale bar 500 nm. **(C)** Analysis of AQP1-positive fibroblasts penetrating into lamina propria tissues. Scale bar 1 μm.

Downloaded from http://chemse.oxfordjournals.org/ at Changhua Christian Hospital on October 6, 2012

left), again indicating high specificity of the AQP1 antibody. The presence of olfactory axon bundles everywhere situated close to Bowman's glands complicated the analysis as the water transport pathway could also be hypothesized to serve the axonal bundles. However, Bowman's glands situated immediately adjacent to bone could also be seen to be surrounded by several layers of fine fibroblast processes labeled for AQP1 (Figure S3A, arrows), arguing that these processes indeed serve the Bowman's glands. Interestingly, while the large venules close to the epithelium always exhibited abundant AQP1 labeling, blood vessels in the deeper regions of the lamina propria, for example, arterioles, had little or no AQP1 labeling (Figure S3B).

Discussion

The olfactory epithelium is potentially vulnerable to dehydration by the inspiratory air stream. In particular, the ion gradients and depolarization activation of the cilia of the olfactory sensory neurons would be vulnerable to evaporation and increased concentration of ions in the airway surface liquid. Olfaction deficiencies were recently predicted and subsequently demonstrated in the AQP4 knockout mouse (Sorbo et al. 2007; Lu et al. 2008). The aquaporin pathways we have described here, as summarized in Figure 5, immediately suggest a possible mechanism for homeostatic balance. Loss of water to evaporation would lead to the creation of an osmotic gradient by the remaining ions, upon which the aquaporin pathway would rapidly restore the equilibrium by water transport and thus protect the neuronal function.

The mucins we have found in the Bowman's glands probably participate in the general mucus layer protection against infectious agents and particles. However, because the olfactory sensory neuron cilia are known to be nonmotile, the olfactory mucosa might not be as well protected from infections as the respiratory epithelium. Thus, two mechanisms for

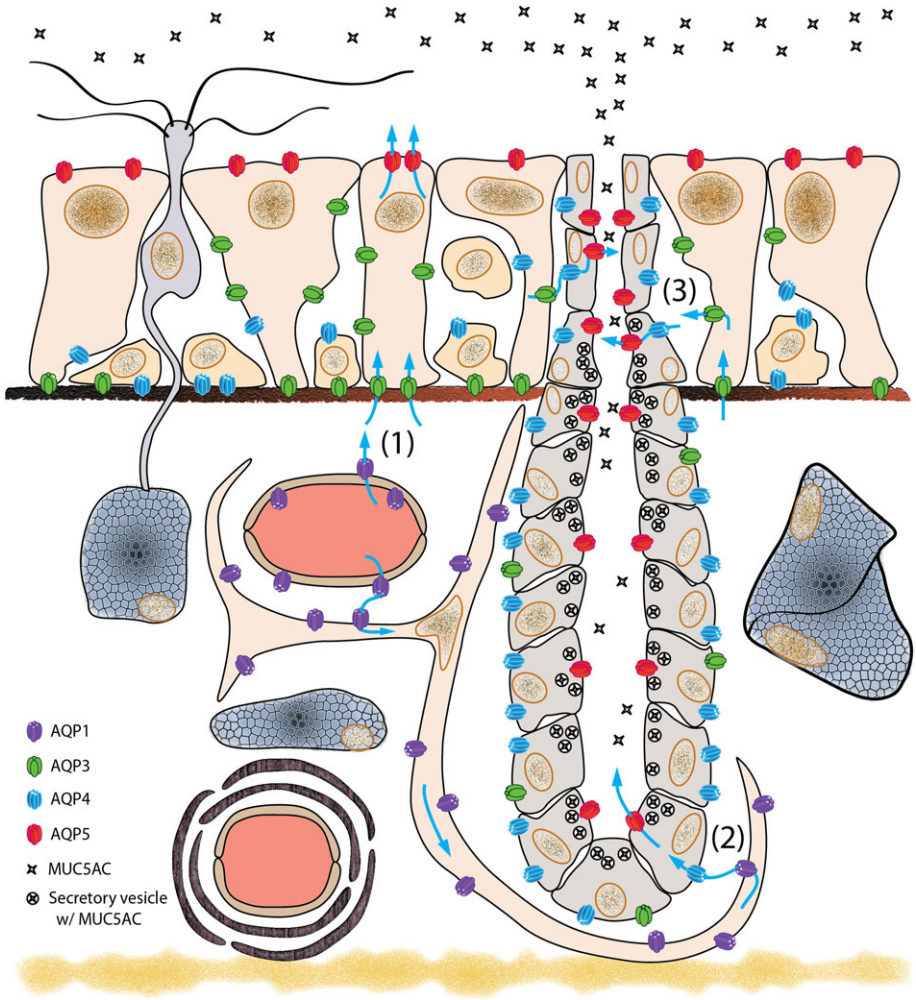

Figure 5 The waterways from blood to the olfactory epithelium surface. Summary diagram of the olfactory mucosa with ciliated olfactory sensory neurons, sustentacular cells, basal cells and duct cells in the olfactory epithelium (top) and lamina propria with axonal bundles, blood vessels, fibroblasts and Bowman's glands laying above the cribriform bone (bottom). The putative water pathways to the airway surface liquid from the large superficial venules are marked by arrows, either directly through the (i) epithelium, through the fibroblast network to the (ii) duct lumen or to the duct lumen from the (iii) epithelium.

Downloaded from http://chemse.oxfordjournals.org/ at Changhua Christian Hospital on October 6, 2012

mucus clearance seem possible. First, the geometric position of the olfactory epithelium dorsally in the nasal cavity could lead to gravitational and centrifugal sliding of the mucus down into the respiratory epithelium where standard ciliary transport could take place. Second, a continual production of mucus from the Bowman's glands—and the strong expansion of mucins alongside rapid water transport—could lead to displacement of mucus. Thus, Bowman's glands might protect the olfactory mucosa against infectious agents both directly and indirectly.

The Bowman's glands of the olfactory mucosa are not well understood and in some details our findings differ from previous studies. Histological and anatomical studies performed in a range of species have showed that some species have serous or mucous glands or both (Getchell and Getchell 1992). However, we find that rats and mice only have mucous Bowman's glands, as is also the case in bats (Yamamoto 1976).

The exact secretion products of Bowman's glands have long remained unidentified. We show that the mucin MUC5AC is present in the Bowman's glands secretory cells, in ducts, and on the surface of the olfactory epithelium and thus represent the first identified mucous product from Bowman's glands. Bowman's glands might also produce other mucins, such as MUC5B, known to be the primary secretory component of submucosal glands in the lower airways (Rose and Voynow 2006). Other secretion products from the Bowman's glands are presently not known, but enzyme assays have indicated that one or more of the at least 14 different carbonic anhydrase family members are present in guinea pig Bowman's glands and ducts (Okamura et al. 1999). On an analogy with the CFTR-regulated cotransport of bicarbonate and chloride in other submucosal glands (Song and Verkman 2001), we tested, but found, no presence of CFTR in Bowman's glands. Thus, the driving force for water and mucin secretion remains unknown.

AQP4 is strongly present in the basolateral sides of Bowman's glands acinar cells and thus participates in a water pathway into these glands. On the other hand, the goblet cells of the respiratory epithelium had distinctly lower AQP4 expression level than the surrounding respiratory epithelial cells, showing that mucus secretion and water transport might not be directly linked. Interestingly, a study on single glands from cystic fibrosis patients found that ion concentrations of mucous glands secretions were similar to normal controls, but that the mucus concentration was higher (Jayaraman et al. 2001), indicating both that mucus does not contribute significantly to the osmotic force and also that mucus and ion secretion must be coregulated upstream of the CFTR regulator.

AQP1 was found by immunogold analysis to be abundantly present in the large venules close to the epithelium but, interestingly, absent from several types of other blood vessels, including the deep arterioles and other capillaries and venules distal to the epithelium. Extremely thin, long processes of fibroblasts, on the other hand, were found to express high levels of AQP1 and to penetrate deep into tissues to surround Bowman's glands. The intricate organization of water channels in the superficial large venules, fibroblasts and Bowman's glands indicates that a water supply pathway is necessary for the function of the Bowman's glands. Rash and coworkers have demonstrated the presence of abundant connexin-43 gap junctions between fibroblasts in the olfactory mucus (Rash et al. 2005). Possibly fibroblasts might form a continuous fibroblast syncytium, similar to the glial syncytium in the brain (Rash et al. 1997), in order to support Bowman's gland function.

How Bowman's glands and aquaporins in the olfactory mucosa are regulated is not known, but parasympathetic constriction of the air stream correlates with increased secretion (Slome 1955; Malcomson 1959). Sympathetic stimuli lead to shrinkage and reduced secretion, conditions under which increased airflow could aggravate the risk to the olfactory epithelium. In recovering rhinitis medicamentosa patients, who have overused nasal sprays for long periods of time, no loss of sense of smell have been reported (Graf 2007), which indicates that protective systems exist in the olfactory mucosa. Thus, the secretion and airway surface liquid production of the olfactory mucosa could be predicted to be inversely regulated with respect to the respiratory epithelium. One study of salamander Bowman's glands reported fewer secretory vesicles upon adrenergic agonist injection (Zielinski et al. 1989), which would indicate sympathetic regulation of olfactory mucus secretion in amphibians.

Supplementary material

Supplementary Figures S1–S3 can be found at http://www.chemse.oxfordjournals.org/.

Funding

Functional Genomics program of the Norwegian Research Council.

Acknowledgements

We thank Dr Toshiyuki Matsuzaki for the gift of the RaTM14 and RaTM41 AQP5 antibodies. We thank Dr Soren Nielsen for the AQP1 antibody. We thank Bjørg Riber for excellent technical assistance with electron microscopy blocks. We thank Carina Knudsen for graphical design. We thank Line Strand, Eystein Hoddevik, Michael R. Daws, and Per Brodal for comments upon the manuscript.

References

Ablimit A, Matsuzaki T, Tajika Y, Aoki T, Hagiwara H, Takata K. 2006. Immunolocalization of water channel aquaporins in the nasal olfactory mucosa. Arch Histol Cytol. 69:1–12.

Bojsen-Moller F. 1964. Topography of the nasal glands in rats and some other mammals. Anat Rec. 150:11–24.

Downloaded from http://chemse.oxfordjournals.org/ at Changhua Christian Hospital on October 6, 2012

Breipohl W. 1972. Licht- under elektronenmikroskopische Befunde zur Struktur der Bowmanschen Drüsen im Riechepithel der weissen Maus. Z Zellforsch Mikrosk Anat. 131:329–346.

Chaudhry FA, Lehre KP, van Lookeren CM, Ottersen OP, Danbolt NC, Storm-Mathisen J. 1995. Glutamate transporters in glial plasma membranes: highly differentiated localizations revealed by quantitative ultrastructural immunocytochemistry. Neuron. 15:711–720.

Cuschieri A, Bannister LH. 1974. Some histochemical observations on the mucosubstances of the nasal glands of the mouse. Histochem J. 6: 543–558.

Frisch D. 1967. Ultrastructure of mouse olfactory mucosa. Am J Anat. 121:87–120.

Getchell ML, Getchell TV. 1992. Fine structural aspects of secretion and extrinsic innervation in the olfactory mucosa. Microsc Res Tech. 23: 111–127.

Graf PM. 2007. Rhinitis medicamentosa. Clin Allergy Immunol. 19:295–304.

Jayaraman S, Joo NS, Reitz B, Wine JJ, Verkman AS. 2001. Submucosal gland secretions in airways from cystic fibrosis patients have normal [Na(+)] and pH but elevated viscosity. Proc Natl Acad Sci U S A. 98:8119–8123.

Kamijo A, Terakawa S, Hisamatsu K. 1993. Neurotransmitter-induced exocytosis in goblet and acinar cells of rat nasal mucosa studied by video microscopy. Am J Physiol. 265:L200–L209.

Katz S, Merzel J. 1977. Distribution of epithelia and glands of the nasal septum mucosa in the rat. Acta Anat. 99:58–66.

King LS, Kozono D, Agre P. 2004. From structure to disease: the evolving tale of aquaporin biology. Nat Rev Mol Cell Biol. 5:687–698.

Klaassen AB, Kuijpers W, Denuce JM. 1981. Morphological and histochemical aspects of the nasal glands in the rat. Anat Anz. 149:51–63.

Köllicker A. 1855. Handbuch der Gewebelehre des Menschen. Leipzig (Germany): Engelmann.

Lu DC, Zhang H, Zador Z, Verkman AS. 2008. Impaired olfaction in mice lacking aquaporin-4 water channels. FASEB J. 22:3216–3223.

Ma T, Song Y, Gillespie A, Carlson EJ, Epstein CJ, Verkman AS. 1999. Defective secretion of saliva in transgenic mice lacking aquaporin-5 water channels. J Biol Chem. 274:20071–20074.

Madrid R, Le MS, Barrault MB, Janvier K, Benichou S, Merot J. 2001. Polarized trafficking and surface expression of the AQP4 water channel are coordinated by serial and regulated interactions with different clathrin-adaptor complexes. EMBO J. 20:7008–7021.

Malcomson KG. 1959. The vasomotor activities of the nasal mucous membrane. J Laryngol Otol. 73:73–98.

Matsuzaki T, Ablimit A, Suzuki T, Aoki T, Hagiwara H, Takata K. 2006. Changes of aquaporin 5-distribution during release and reaccumulation of secretory granules in isoproterenol-treated mouse parotid gland. J Electron Microsc. 55:183–189.

Menco BP, Bruch RC, Dau B, Danho W. 1992. Ultrastructural localization of olfactory transduction components: the G protein subunit Golf alpha and type III adenylyl cyclase. Neuron. 8:441–453.

Nakashima T, Kimmelman CP, Snow JB, Jr. 1984. Structure of human fetal and adult olfactory neuroepithelium. Arch Otolaryngol. 110:641–646.

Neely JD, Amiry-Moghaddam M, Ottersen OP, Froehner SC, Agre P, Adams ME. 2001. Syntrophin-dependent expression and localization of Aquaporin-4 water channel protein. Proc Natl Acad Sci U S A. 98:14108–14113.

Nielsen S, King LS, Christensen BM, Agre P. 1997a. Aquaporins in complex tissues. II. Subcellular distribution in respiratory and glandular tissues of rat. Am J Physiol. 273:C1549–C1561.

Nielsen S, Nagelhus EA, Amiry-Moghaddam M, Bourque C, Agre P, Ottersen OP. 1997b. Specialized membrane domains for water transport in glial cells: high-resolution immunogold cytochemistry of aquaporin-4 in rat brain. J Neurosci. 17:171–180.

Nielsen S, Smith BL, Christensen EI, Agre P. 1993. Distribution of the aquaporin CHIP in secretory and resorptive epithelia and capillary endothelia. Proc Natl Acad Sci U S A. 90:7275–7279.

Okamura H, Sugai N, Suzuki K. 1999. Localization of carbonic anhydrase in guinea pig Bowman's glands. J Histochem Cytochem. 47: 1525–1532.

Rash JE, Davidson KG, Kamasawa N, Yasumura T, Kamasawa M, Zhang C, Michaels R, Restrepo D, Ottersen OP, Olson CO, et al. 2005. Ultrastructural localization of connexins (Cx36, Cx43, Cx45), glutamate receptors and aquaporin-4 in rodent olfactory mucosa, olfactory nerve and olfactory bulb. J Neurocytol. 34:307–341.

Rash JE, Duffy HS, Dudek FE, Bilhartz BL, Whalen LR, Yasumura T. 1997. Grid-mapped freeze-fracture analysis of gap junctions in gray and white matter of adult rat central nervous system, with evidence for a "panglial syncytium" that is not coupled to neurons. J Comp Neurol. 388: 265–292.

Rogers DF. 1994. Airway goblet cells: responsive and adaptable front-line defenders. Eur Respir J. 7:1690–1706.

Rose MC, Voynow JA. 2006. Respiratory tract mucin genes and mucin glycoproteins in health and disease. Physiol Rev. 86:245–278.

Schwob JE. 2002. Neural regeneration and the peripheral olfactory system. Anat Rec. 269:33–49.

Seifert K. 1971. Licht- und elektronenmikroskopische Untersuchungen der Bowman-Drüsen in der Riechschleimhaut makrosmatischer Säuger. Arch Klin Exp Ohren Nasen Kehlkopfheilkd. 200:252–274.

Slome D. 1955. Physiology of nasal circulation. Lect Sci Basis Med. 5:451–468.

Song Y, Verkman AS. 2001. Aquaporin-5 dependent fluid secretion in airway submucosal glands. J Biol Chem. 276:41288–41292.

Sorbo JG, Moe SE, Holen T. 2007. Early upregulation in nasal epithelium and strong expression in olfactory bulb glomeruli suggest a role for aquaporin-4 in olfaction. FEBS Lett. 581:4884–4890.

Tandler B, Bojsen-Moller F. 1978. Ultrastructure of the anterior medial glands of the rat nasal septum. Anat Rec. 191:147–167.

Thrane AS, Rappold PM, Fujita T, Torres A, Bekar LK, Takano T, Peng W, Wang F, Thrane VR, Enger R, et al. 2011. Critical role of aquaporin-4 (AQP4) in astrocytic Ca2+ signaling events elicited by cerebral edema. Proc Natl Acad Sci U S A. 108:846–851.

Todd RB, Bowman W. 1847. The physiological anatomy and physiology of man. London: Parker & Son.

Yamamoto M. 1976. An electron microscopic study of the olfactory mucosa in the bat and rabbit. Arch Histol Jpn. 38:359–412.

Zielinski BS, Getchell ML, Wenokur RL, Getchell TV. 1989. Ultrastructural localization and identification of adrenergic and cholinergic nerve terminals in the olfactory mucosa. Anat Rec. 225:232–245.

Downloaded from http://chemse.oxfordjournals.org/ at Changhua Christian Hospital on October 6, 2012